Naval Research Laboratory

Washington, DC 20375-5000

NRL Memorandum Report 6584

Pseudo-Steady Diffusional Growth or Collapse of Bubbles Rising in Time Dependent Pressure Fields

M. CERZA,* O.M. GRIFFIN AND M.B. STEWART

Laboratory for Computational Physics and Fluid Dynamics

**David Taylor Research Center*
Bethesda, MD 20084-5000

March 13, 1990

REPORT DOCUMENTATION PAGE

Form Approved
OMB No. 0704-0188

1. AGENCY USE ONLY *(Leave blank)*	2. REPORT DATE	3. REPORT TYPE AND DATES COVERED
	1990 March 13	Final

4. TITLE AND SUBTITLE

Pseudo-Steady Diffusional Growth or Collapse or Bubbles Rising in Time-Dependent Pressure Fields

5. FUNDING NUMBERS

PE - 61153N
TA - RR023-01-41

6. AUTHOR(S)

Cerza,* M., Griffin, O.M. and Stewart, M.B.

7. PERFORMING ORGANIZATION NAME(S) AND ADDRESS(ES)

Naval Research Laboratory
Washington, DC 20375-5000

8. PERFORMING ORGANIZATION REPORT NUMBER

NRL Memorandum Report 6584

9. SPONSORING/MONITORING AGENCY NAME(S) AND ADDRESS(ES)

Office of Naval Research
Arlington, VA 22217

10. SPONSORING/MONITORING AGENCY REPORT NUMBER

11. SUPPLEMENTARY NOTES

*David Taylor Research Center
Bethesda, MD 20084-5000

12a. DISTRIBUTION/AVAILABILITY STATEMENT

Approved for public release; distribution unlimited.

12b. DISTRIBUTION CODE

13. ABSTRACT *(Maximum 200 words)*

A pseudo-steady convective model for bubble diffusional growth or collapse while rising in time dependent pressure fields has been developed. The bubble model assumes the neglect of added mass, history, and interfacial momentum terms. Criteria are developed to show when these terms affect the bubble motion. The pressure fields investigated are a simple hydrostatic head, a decompression hydrostatic head, and a hydrostatic head with the oscillation of the reference pressure (atmosphere above the hydrostatic head).

Keywords: diffusion equations, velocity profiles, bubble motion

14. SUBJECT TERMS

Bubble dynamics, Fluid dynamics, (KR)
Ship wakes

15. NUMBER OF PAGES 35

16. PRICE CODE

17. SECURITY CLASSIFICATION OF REPORT	18. SECURITY CLASSIFICATION OF THIS PAGE	19. SECURITY CLASSIFICATION OF ABSTRACT	20. LIMITATION OF ABSTRACT
UNCLASSIFIED	UNCLASSIFIED	UNCLASSIFIED	UL

NSN 7540-01-280-5500

Standard Form 298 (Rev. 2-89)
Prescribed by ANSI Std. Z39-18
298-102

CONTENTS

NOMENCLATURE v

INTRODUCTION 1

GENERAL EQUATIONS 2

VELOCITY PROFILES AND BUBBLE MOTION 6

SOLUTION 8

RESULTS 12

VALIDITY OF THE PSEUDO-STEADY MODEL 25

CONCLUSIONS 29

ACKNOWLEDGEMENTS 29

REFERENCES 30

NOMENCLATURE

English

a	radius at bubble wall
C	species concentration
d	bubble diameter
D	Diffusion coefficient
f	frequency, Hz
g	gravity constant
H(t)	arbitrary function of time
m	mass
P	pressure
ΔP	pressure amplitude
r	radial coordinate
R	gas constant
t	time
T	temperature
U	velocity
V	bubble volume
x	bubble translational distance
Pe	Peclet number, $\frac{aU_b}{D}$
Re	Reynolds number, $\frac{2aU_b}{\nu}$
Sh	Sherwood number, see eq. (33)

Greek

γ	specific weight
δ	diffusion thickness
ϵ	δ^2
θ	angular coordinate
μ	dynamic viscosity
ν	kinematic viscosity
ρ	density
τ	time constant or dummy variable
ψ	stream function or diffusion parameter

Subscripts

b	bubble
B	Bottom, start of bubble rise
f	fluid
r	radial component
s	saturation
θ	tangential component
∞	ambient

PSEUDO-STEADY DIFFUSIONAL GROWTH OR COLLAPSE OF BUBBLES RISING IN TIME DEPENDENT PRESSURE FIELDS

INTRODUCTION

The growth or collapse of bubbles, whether they be comprised of the vapor of the surrounding ambient fluid or of an entirely different species, has led rise to some very significant phenomena. Examples of which, to name a few, are nucleate boiling in pools and thin liquid films, cavitation, bubble formation in molding processes, entrainment from breaking waves and jets, and bubble persistence in the wakes of ships. Vapor bubble generation and growth, though very important to the field of nucleate boiling heat transfer, will be discarded as a topic for this report and, instead, concentration will be focused on the growth or collapse of bubbles due to mass transfer between the bubble species and the surrounding fluid.

One of the first formulations of bubble diffusion was that of Epstein and Plesset [1] in which the mass transfer from a stationary bubble was examined. A bubble was shown to either grow or collapse depending on whether the ambient fluid was either oversaturated or undersaturated, respectively, with the species that comprised the bubble. Other significant analyses of this problem can be found in the works of Kirkaldy [2], Scriven [3], and Goodrich [4], to name a few. Early experimental studies of diffusion controlled growth or collapse have been conducted by Haughton, et al. [5], Wise and Haughton [6,7], and Krieger, et al. [8] in which dissolving spherical gas bubbles were studied in order to determine diffusion coefficients. In those studies the bubbles were attached to a solid wall or capillary so that they were stationary. Gowing [9] in a more recent study also examined the dissolving characteristies of bubbles affixed to electrodes. In Gowing's study,both sea water and distilled water were used as the dissolving medium.

Ruckenstein [10], in a very eloquent solution, showed that if a bubble were moving, translation would have a very pronounced effect on diffusion. Even for small bubble velocities, convective diffusion would supply a very large portion of a bubble's collapse rate, assuming that the bubble is moving in an undersaturated ambient fluid. In this model the effect of the bubble's radial velocity was neglected. Ruckenstein and Davis [11] then extended the analysis in [10] to cover the case where the bubble radial velocity is important, such as the case when either a high concentration gradient exists at the bubble wall or the ambient fluid has very high diffusion coefficient. Under these conditions, the bubble wall may be moving at the same order of magnitude as the bubble translational velocity in which case the radial velocity becomes important. In both models, the bubble is assumed to be moving at a steady velocity and the surrounding pressure field is assumed constant.

Recent experimental data for bubbles rising in a liquid have been taken by Brankovic, et al. [12], Ishikawa, et al. [13] and Payvar [14] to name a few. Brankovic, et al. collected data for air and carbon dioxide bubbles with a triple-peak laser Doppler technique. The bubbles, which were on the order of 0.25 to 1.2mm in diameter, displayed the typical very quick acceleration to some maximum velocity, then a decrease in terminal velocity as they continued to rise. For the smaller bubbles, this velocity decrease reached a steady velocity, but for the larger bubbles the velocity decrease continued throughout the measurement length of the test section, 12cm. This transition to lower velocities was partially explained by the presence in the liquid of surfactants which have a tendency to accumulate on the

Manuscript approved December 18, 1989.

bubble skin and increase the bubble's drag by freezing the interfacial motion between the bubble and its surrounding fluid. Drag coefficient and Sherwood number as functions of Reynolds and Peclet numbers, respectively, were also shown.

Ishikawa, et al. [13] measured the rise velocity for $60-1170\mu m$ carbon dioxide bubbles in water and aqueous sucrose solutions via a photographic method. Their results agreed well with theoretical and empirical equations for rigid spheres in creeping flow for d_B less than $150\mu m$ and began to approach the solutions for clean fluid spheres as d_B increased, though partial contamination did occur. In their data reduction, they did take into account bubble volumetric expansion through its rise in a hydrostatic pressure field.

Payvar [14] examined the effects, both experimentally and analytically, of a rapid decompression on bubble growth for CO_2 bubbles in ethyl alchohol. In this study the bubble was assumed to be stationary and the diffusive boundary layer around it was assumed constant. Predicted results were in good agreement with experimental measurements. The initial pressure range at the start of the decompression was 0.44-1.12MPa.

The purpose of this theoretical study is to examine the effects on mass transfer of a bubble rising in a hydrostatic pressure field and undergoing various time dependent pressure fluctuations. To date, there have been no mathematical models for a translational bubble rising through such fields. Furthermore, bubble experimental rise data have only been obtained for a static hydrostatic head, with the exception of Payvar [14], but that was for a stationary bubble. This paper will focus on pseudo-steady bubble translation as a first attack on these types of problems. The pseudo-steady analysis will hold when bubble acceleration through the pressure field is negligible. Three types of pressure fields will be examined: 1) a simple hydrostatic head; 2) a compression/decompression hydrostatic head; and 3) an oscillating pressure field imposed on a hydrostatic head. The mathematical model will entail extending the model of Ruckenstein and Davis [11] to cover time dependent pressure fields imposed on hydrostatic heads.

GENERAL EQUATIONS

The problem to be considered will be a single component bubble rising vertically in a liquid (Fig. 1). The liquid maintains a hydrostatic head and a time dependent pressure field may or may not be present. A rising bubble would therefore exhibit a volumetric change due to the change in ambient pressure it encounters and if there is any mass transfer via diffusion a second term for volumetric change would also be apparent. This can readily be expressed by differentiation of the perfect gas law as

$$\frac{1}{V}\frac{dV}{dt} = \frac{1}{m_b}\left[\frac{dm_b}{dt} - \frac{V}{RT}\frac{dP}{dt}\right]. \tag{1}$$

The first term on the right represents the volumetric change due to mass loss or gain and can be found by first solving the equation for convective diffusion in the fluid surrounding the bubble, then finding the gradient of concentration at the bubble wall and finally integrating the concentration gradient over the bubble surface to find the total mass transfer. The second term represents the volumetric change the bubble undergoes as it travels through the external pressure field. The diffusion equation can be represented as

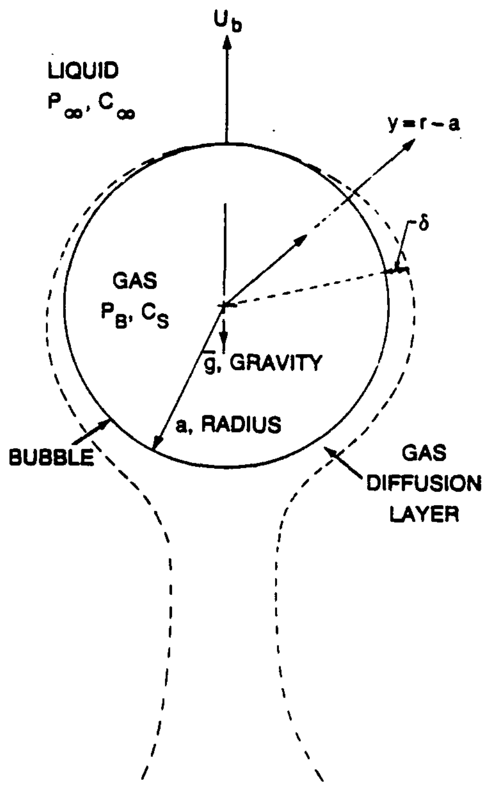

Figure 1. Bubble Configuration.

$$\frac{\partial C}{\partial t} + U_r \frac{\partial C}{\partial r} + \frac{U_\theta}{r}\frac{\partial C}{\partial \theta} = \frac{D}{r^2}\frac{\partial}{\partial r}\left(r^2 \frac{\partial C}{\partial r}\right), \tag{2}$$

subject to the following conditions,

$$at \quad r =_\infty, C = C_o, t > 0, \tag{3a}$$

$$at \quad r = a, C = C_s, t > 0, \tag{3b}$$

and

$$at \quad t = 0, C = C_o, all\ r > a. \tag{3c}$$

Furthermore, if the diffusion coefficient is small such that the diffusion penetration depth is much less than the bubble radius the term on the right can be expanded and reduced, i.e.

$$\frac{\partial^2 C}{\partial r^2} >> \frac{2}{r}\frac{\partial C}{\partial r}.$$

The result is

$$\frac{\partial C}{\partial t} + U_r \frac{\partial C}{\partial r} + \frac{U_\theta}{r}\frac{\partial C}{\partial \theta} = D\frac{\partial^2 C}{\partial r^2}. \tag{2a}$$

From Scriven [3] the mass transfer rate at the bubble wall is

$$\frac{dm}{dt} = 2\pi a^2 D \int_o^{\pi} \left(\frac{\partial C}{\partial r}\right)_{r=a} sin\theta d\theta \tag{4}$$

where molal effects due to dissolving species have been neglected. Continuity in the fluid surrounding the bubble can best be employed by the use of the stream function, ψ as,

$$U_r = \frac{1}{r^2 \sin\theta} \frac{\partial \psi}{\partial \theta} \tag{5a}$$

and

$$U_\theta = -\frac{1}{r sin\theta} \frac{\partial \psi}{\partial r} \tag{5b}$$

This then implies the use of axial symmetry on the rising bubble.

The radial and tangential velocities in eq. (2) and (5) can be found from the solution to the transient stream function equation,

$$E^2\left(E^2 - \frac{1}{\nu}\frac{\partial}{\partial t}\right)\psi = 0 \tag{6}$$

where

$$E^2 \equiv \frac{\partial^2}{\partial r^2} + \frac{sin\theta}{r^2}\frac{\partial}{\partial \theta}\left(\frac{1}{sin\theta}\frac{\partial}{\partial \theta}\right)$$

It should be noted that in eq. (6) the convective acceleration terms have been omitted since we are considering transient creeping flow. This is a good assumption considering the proposed slow acceleration changes of the bubble. The boundary conditions to equation (6) with respect to axes fixed at the instantaneous bubble center are

$$\psi, U_r, U_\theta = finite \quad as \quad r \rightarrow \infty, \tag{7a}$$

$$\left.\frac{1}{sin\theta}\frac{\partial \psi}{\partial \theta}\right)_{r=a} = U_b a^2 cos\theta + a^2 \frac{da}{dt}, \tag{7b}$$

$$\left[-r\frac{\partial}{\partial r}\left(\frac{1}{r^2 sin\theta}\frac{\partial \psi}{\partial r}\right) + \frac{1}{r}\frac{\partial}{\partial \theta}\left(\frac{1}{r^2 sin\theta}\frac{\partial \psi}{\partial \theta}\right)\right]_{r=a} = 0, \tag{7c}$$

and

$$\psi = 0 \quad at \quad t = 0. \tag{7d}$$

Equation (7c) applies for the case of a fluid sphere. It is a suspected fact that surfactant contamination does effect the motion of the rising bubble by stopping the movement of the bubble interfacial surface, thus, causing the bubble to behave like a solid particle; however, this hypothesis is not investigated in this theory.

Notice that in boundary condition (7b), the bubble velocity is present. In general it cannot be assumed constant, hence, it can be obtained through the law of Lagrangian motion, which can be written for the bubble as

$$\frac{\partial}{\partial t}\left(m_b U_b\right) = -\pi\mu \int_0^\pi \left[r^4 sin\theta\left(\frac{E^2\psi}{r^2}\right)\right]_{r=a} d\theta$$

$$+\rho_f\pi \int_0^\pi \left[\frac{\partial}{\partial r}\left(\frac{\partial\psi}{\partial t}\right)r^2\right]_{r=a} sin\theta \;\; d\theta + \rho_f\frac{4}{3}\pi a^3 g. \tag{8}$$

The left hand side of eq. (8) represents the time rate of momentum change for a drop or bubble. In the case of a gaseous bubble in a heavy liquid, it is generally very small. The first term on the right side represents the steady normal and tangential forces that the fluid exerts on the bubble. The derivation of the format for this term can be found in Happel and Brenner [15]. The transient second term on the right, again from [15], represents the change in momentum due to added mass, "history" or Basset - Boussinesq - Oseen (B-B-O) term, and (in the case of a fluid sphere) the momentum required to change the motion of the bubble-fluid interface. Finally, the third term is due to buoyancy, here, only the density of the fluid is retained since it is assumed that the fluid is much heavier than the gas.

The second term in eq. (1) represents the volumetric change due to surrounding pressure. If the hydrostatic pressure can be expressed as

$$P = P_B - \gamma x, \tag{9}$$

where P_B = the pressure at the depth where a bubble is first released, then

$$\frac{dP}{dt} = -\gamma\frac{dx}{dt} = -\gamma U_b. \tag{10}$$

Hence, for the case of a bubble rising in a simple hydrostatic pressure field, the rate of change of pressure that the bubble encounters is directly proportional to the bubble rise velocity. Consider now a bubble rising in a fluid that is undergoing a compression/depression pressure field which can be caused by the charging or venting of the atmosphere above the water column to a desired pressure differential. The pressure field can be expressed as

$$P = P_B + \triangle P e^{\;\pm t/\tau} - \gamma x \tag{9a}$$

where $\triangle P$ = desired pressure differential, and τ = time constant. It then follows that

$$\frac{dP}{dt} = \pm\frac{\triangle P e^{\pm t/\tau}}{\tau} - \gamma U_b. \tag{10a}$$

An imposed sinusoidal oscillation on the hydrostatic field can, likewise, be expressed as

$$P = P_B + \Delta P sin(2\pi f t) - \gamma x \tag{9b}$$

where

$$f = \text{ oscillation frequency, } H_z$$

Then

$$\frac{dP}{dt} = 2\pi f \Delta P cos(2\pi f t) - \gamma U_b \tag{10b}$$

In general if we can express any time dependent field mathematically, i.e., Fourier series, complex series, etc, we can then take the first derivative with respect to time and utilize it in eq. (1).

The equations thus developed represent a system of equations that is, in general, both coupled and non-linear. The non-linearity arising from the fact that the radial boundary condition for the stream function is a non-linear function of the bubble radius which in turn is coupled through the convective diffusion equation. Thus, a general solution procedure would entail the solution of eqs. (1) through (10) simultaneously, which is beyond the scope of this first presentation. We shall restrict ourselves to the solution of pseudo-steady problems which, as we shall see, will decouple the system of equations and reduce the issue of non-linearity to a very weak one.

VELOCITY PROFILES AND BUBBLE MOTION

In the following solution, the prevailing assumptions that reduce the system of equations to a pseudo-steady set are:

1) the bubble accelerational changes are small,

and

2) the bubble radial growth/collapse rate is small.

The above assumptions allow us to linearize eqs. (6) and (7) into the following superpositioned form

$$\psi = \psi_{\substack{translation \\ a=constant}} + \psi_{\substack{radial \\ a=variable}} \tag{11}$$

The first part of eq. (11) has been solved by the method of Laplace transforms and for a no-slip boundary condition eq. (8) becomes

$$\begin{aligned} \frac{\partial}{\partial t}\left(m_b U_b\right) &= -\frac{m_f}{2}\frac{dU_b}{dt} - 6\pi\mu a U_b \\ &\quad - \frac{9m_f}{2a}\sqrt{\frac{\nu}{\pi}}\int_0^t \frac{dU_b/d\tau}{\sqrt{t-\tau}}d\tau + m_f g. \end{aligned} \tag{12}$$

The first term on the right represents the added mass loading, the second term is the Stokesian drag, the third term represents that obtained by Basset [16], and the fourth is the bouyant force. For the case of a bubble, Morrison and Stewart [17] solved eq. (8) shown here assuming no transient external forces,

$$\frac{\partial}{\partial t}(m_b U_b) = 0 = -\frac{m_f}{2}\frac{dU_b}{dt} - 4\pi\mu a U_b - \frac{3m_f}{a}\sqrt{\frac{\nu}{\pi}}\int_0^t \frac{dU_b/d\tau}{\sqrt{t-\tau}}d\tau$$

$$-\frac{m_f a}{6\sqrt{\pi\nu}}\int_0^t \frac{d^2U_b/d\tau^2}{\sqrt{t-\tau}}d\tau + m_f g. \tag{13}$$

Here, the drag and history terms are altered by a constant, and the fourth term represents the momentum required to move the bubble interface during changes of acceleration. For the case of a gaseous bubble undergoing negligible acceleration changes in a heavy fluid. eqs. (12) and (13) reduce to

$$U_b = C(g/\nu)a^2(t), \tag{14}$$

where the constant

$$C = \begin{cases} 1/3, & \text{for slip flow, Re<1;} \\ 2/9, & \text{for no-slip, Re<1; and} \\ 1/9, & \text{for viscous dissipation, Re>>1.} \end{cases} \tag{14a}$$

The potential flow solution with viscous dissipation by Levich [18] was here added for later comparisons. Since bubble acceleration is assumed small, eq. (14) is representative of the Hadamard-Rybczynski solution for a bubble [19, 20]; the velocity profiles relative to a stopped bubble center, are

$$U_r = \left[\left(U_o - \frac{U_b}{2}\right)\frac{a^3}{r^3} + \left(\frac{3}{2}U_b - U_o\right)\frac{a}{r} - U_b\right]cos\theta \tag{15a}$$

and

$$U_\theta = \left[\left(\frac{U_o}{2} - \frac{U_b}{4}\right)\frac{a^3}{r^3} + \left(\frac{U_o}{2} - \frac{3}{4}U_b\right)\frac{a}{r} + U_b\right]sin\theta \tag{15b}$$

where

$$U_o = \frac{U_b}{2(1+\mu_g/\mu_f)}.$$

The second term on the right of eq. (11) represents the stream function for the pure radial motion of a stopped bubble. Consequently, there are no fluid forces on the bubble for pure radial motion, hence this term does not add to the fluid loading on the bubble through eq. (8). This can readily be verified through eq. (8) since

$$\psi_{\substack{radial\\ amvariable}} = -a^2(da/dt)cos\theta. \tag{16}$$

Thus, eqs. (12) and (13) remain intact. The radial stream function does, however, add a component to the velocity profile in eq. (15a) of

$$\frac{a^2}{r^2}\left(\frac{da}{dt}\right).$$

Hence, eq. (15a) becomes

$$U_r = \left[\left(U_0 - \frac{U_b}{2}\right)\frac{a^3}{r^3} + \left(\frac{3}{2}U_b - U_0\right)\frac{a}{r} - U_b\right]cos\theta + \frac{a^2}{r^2}\left(\frac{da}{dt}\right). \tag{17}$$

SOLUTION

Eq. (1) shows that the radial history for the rising bubble can be expressed as

$$\frac{da}{dt} = \frac{a}{3m_b}\left[\frac{dm_b}{dt} - \frac{V}{RT}\frac{dP}{dt}\right]. \tag{18}$$

The first term in the brackets on the right side of eq. (18) can then be found by utilizing the solution of Ruckenstein and Davis [11] for diffusion controlled growth of a bubble moving at a steady velocity, and slowly changing mass. This solution seems applicable for most gases in water where there exists moderate concentration gradients at the bubble wall and small diffusion coefficients. It is not the intent of this paper to repeat the eloquent solution by Ruckenstein and Davis [11], only to show that their model can be utilized for problems of time dependent pressure fields imposed on a bubble rising in a hydrostatic head. Restrictions to the use of their model are limited when one of the following occur:

1) density differences in the two fluids allow a significantly long duration bubble acceleration profile;
2) the time dependent pressure field is able to make large volumetric expansions, in which case large bubble accelerations will be present;
3) the diffusion process is large enough to force large changes in bubble radius through mass loss/gain, thus allowing significant bubble acceleration:

and

4) the time dependent pressure field varies rapidly, such as high frequency acoustic waves or sudden explosions in which case bubble radial inertial effects will be present which are neglected in this model.

Ruckenstein and Davis [11] solved eq. (2a) subject to eq. (3) for various velocity profiles by first employing the change in variables that shifts the coordinate system from a moving boundary to one where the frame of reference is fixed at the moving bubble interface, i.e.,

$$y = r - a$$

where y is the diffusion distance from the bubble outward into the fluid (Fig.1). They assumed that this diffusion distance is small compared to the bubble radius, hence eq. (2a) was written for small y/a as

$$\frac{\partial C}{\partial t} - \frac{y}{a}\left(V_r cos\theta + 2\frac{da}{dt}\right)\frac{\partial C}{\partial y} + \frac{V_\theta}{a} sin\theta \frac{\partial C}{\partial \theta} = D\frac{\partial^2 C}{\partial y^2} \tag{19}$$

where

$$V_r = \begin{cases} U_b, & \text{slip-flow, Re<1} \\ 3U_b, & \text{viscous dissipation, Re>>1,} \end{cases} \tag{20a}$$

and

$$V_\theta = \begin{cases} U_b/2, & \text{slip-flow, Re<1} \\ 3U_b/2, & \text{viscous dissipation, Re>>1.} \end{cases} \tag{20b}$$

Ruckenstein and Davis then employed a similarity transformation of the form

$$\eta = \frac{y}{\delta(\theta, t)} \tag{21}$$

which transformed eq (19) into an ordinary differential equation in η in which the constant for the $\frac{dc}{dn}$ term was a functional equation of δ^2. The two resulting equations were then

$$\frac{d^2C}{d\eta^2} + 2\eta\frac{dC}{d\eta} = 0, \tag{22}$$

and

$$\frac{\partial \epsilon}{\partial t} + [\beta(t)cos\theta + \gamma(t)]\epsilon + \alpha(t)sin\theta\frac{\partial \epsilon}{\partial \theta} = 4D, \tag{23}$$

where

$$\epsilon = \delta^2(\theta, t),$$

$$\alpha(t) = \frac{V_\theta}{a},$$

$$\beta(t) = \frac{2V_r}{a},$$

and

$$\gamma(t) = \frac{4}{a}\frac{da}{dt}.$$

After the application of the method of characteristics to eq. (23) their solution for the concentration in the vicinity of the bubble became

$$\frac{C - C_0}{C_s - C_0} = erfc\left[\frac{y}{\delta(\theta, t)}\right] \tag{24}$$

where

$$\delta^2(\theta,t) = 4D\int_0^t exp\int_t^p \left\{ \beta(\xi).\frac{1-[tan^2(\theta/2)]exp[2\int_t^\xi \alpha(s)ds]}{1+[tan^2(\theta/2)]exp[2\int_t^\xi \alpha(s)ds]} + \gamma(\xi)d(\xi)dp \right\}. \quad (25)$$

The mass transfer term of eq. (18) can then be found from

$$\left.\frac{\partial C}{\partial r}\right)_{r=a} = \left.\frac{\partial C}{\partial y}\right)_{y=0} = (C_0 - C_s)\frac{2}{\sqrt{\pi}\delta(\theta,t)} \quad (26)$$

and substituting this result in eq. (4). The solution of eq. (18) through eq. (24) and (25) was found by the present authors to be too time consuming a solution on a small computer for the problem at hand. It was found that by solving eq. (23) in a forward-difference marching scheme for $\delta(\theta, t+dt)$ and, by utilizing this solution for $\delta(\theta,\ t+dt)$, the problem would converge much faster.

The numerical scheme employed was

$$\epsilon(\theta,t) = \delta^2(\theta,t) = \frac{4D + \frac{\alpha(t)sin\theta}{\Delta\theta}\epsilon(t,\theta-d\theta) + \frac{\epsilon(t-dt,\theta)}{\Delta t}}{\left\{\frac{1}{\Delta t} + \frac{\alpha(t)sin\theta}{\Delta\theta} + [\beta(t)cos\theta + \gamma(t)]\right\}}$$

If one assumes a general time dependent pressure field imposed on a hydrostatic head, i.e.,

$$P = P_B + \Delta P H(t) - \gamma x, \quad (27)$$

where H(t) is some time dependency function for the amplitude ΔP, then

$$\frac{dP}{dt} = \Delta P H'(t) - \gamma U_b, \quad (28)$$

some examples of which were given by eq. (10). Eqs. (28), (26) and (18) can then be combined to form

$$\frac{da}{dt} = \frac{a}{3m_b}\left\{4a^2D\sqrt{\pi}(C_0 - C_s)\int_0^\pi \frac{sin\theta}{\delta(\theta,t)}d\theta - \frac{(4/3\pi a^3)}{RT}[\Delta P H'(t) - \gamma U_b]\right\}. \quad (29)$$

The bubble radius at time, t, can then be found from the bubble radius at time $t - dt$ by

$$a_t = a_{t-dt} + \int_{t-dt}^t \left(\frac{da}{dt}\right)dt, \quad (30)$$

which can be evaluated by an integration scheme such as the Trapezoidal or Simpson's rule. The numerical procedure for the solution of eqs. (29) and (30) was as follows:

1) from the previous bubble radius, $\alpha(t), \beta(t)$ and $\gamma(t)$ were calculated and $\delta(\theta, t)$ was found through eq. (23a);
2) da/dt, eq. (29), was then evaluated;
3) a_t was next evaluated through eq. (30);
4) the bubble mass was evaluated through a form similar to eq.(30), utilizing eq. (4);
5) the bubble mass was also independently evaluated from both a_t in 3) and the new bubble density based on surrounding pressure (surface tension effects were not necessary for bubbles larger than $20\mu m$);
6) the mass terms in 5) and 4) were compared. If the comparison was not satisfactory the scheme was reiterated with the new a_t. If the comparison was satisfactory, the time was marched and the process repeated.

Significant Translation

When the bubble translational velocity is much greater than its radial growth velocity, eq. (24) can be greatly simplified by dropping the radial growth term. This can be expected to occur when the gas solubility is small, hence, translational convection predominates. Ruckenstein [10] shows that this simplification results in

$$Sh = (Pe/\pi)^{1/2} w(T) \tag{31}$$

where

$$T = \begin{cases} tU_b/2a, & \text{fluid-sphere, Re<< 1} \\ \frac{3}{2}\frac{tU_b}{a}, & \text{potental flow, Re>>1,} \end{cases}$$

and $w(T)$ =function evaluated in Ref. [10].

When T>>1,w(T)=$4/\sqrt{3}$ and eq. (31) becomes

$$Sh = 4(Pe/3\pi)^{1/2}. \tag{32}$$

Actually,w(T) becomes asymptotic to $4/\sqrt{3}$ as $T > 5$. For rising air bubbles in water, eq. (32) is not a bad approximation of the mass transfer for bubbles greater than about $15\mu m$. By definition,

$$Sh \equiv \frac{2aN}{(C_0 - C_s)D} \tag{33}$$

where

$$N = \frac{dm/dt}{4\pi a^2}.$$

The combination of eqs. (32), (33) and (16) yields the following equation for the bubble mass transfer rate

$$\frac{dm}{dt} = \begin{cases} \frac{8}{\sqrt{6}}(C_0 - C_s)\left[\frac{\pi D g}{\nu}\right]^{1/2} a^{5/2}, & \text{slip-flow, Re<1,} \\ \frac{8}{3\sqrt{2}}(C_0 - C_s)\left[\frac{\pi D g}{\nu}\right]^{1/2} a^{5/2}, & \text{viscous dissipation, Re>>1.} \end{cases} \tag{34}$$

The substitution of eqs. (34), (28) and (16) into eq. (18) yields

$$\frac{da}{dt} = \frac{1}{3m_b}[C_1 a^{7/2} + C_2 a^6 - C_3 H'(t) a^4] \tag{35}$$

where

$$C_1 = \frac{8(C_0 - C_s)}{3\sqrt{2}} \left[\frac{\pi D g}{\nu}\right]^{1/2}$$

$$C_2 = \begin{cases} \frac{4}{9}\frac{\pi g \gamma}{RT\nu}, & \text{slip, Re<1,} \\ \frac{4}{27}\frac{\pi g \gamma}{RT\nu}, & \text{viscous dissipation, Re>>1,} \end{cases}$$

$$C_3 = \frac{4}{3}\frac{\pi \Delta P}{RT}$$

Equation (35) can easily be solved by a fourth order Runge-Kutta routine. All that is needed are the initial conditions a_0, m_{b_0} and the initial pressure.

RESULTS

The results presented are for a bubble rising in a fluid that can undergo pressure changes by means of allowing the atmospheric pressure above the water column to vary in time. Figures 2a-2c depict the diffusion boundary layer shape (as calculated by eq. 29) surrounding air bubbles of radii sizes 0.017, 0.13 and 0.47mm rising in a static water column with an ambient air concentration of 8.2ml/l ($\psi = 3.53$). The respective bubble Reynolds numbers are 0.04, 5.83 and 262. It should be pointed out that eq. 29 does not realistically represent the rise of a 0.47mm radius bubble. The reason for this being that for a bubble of this size, a wake of shedding vortices would exist and the bubble would oscillate and spiral as it rises. Figure 2c should be viewed for comparison purposes only. As can be seen in Figures 2a-2c, the faster the bubble rises the more the diffusion boundary layer is swept back around the bubble and the thinner its "tail" becomes. Across the diffusion layer exists a concentration profile from the fully-saturated air concentration inside the bubble to the ambient air concentration in the fluid outside the diffusion boundary layer. The local diffusion rates of mass transfer around the surface of the bubble are a function of the diffusion layer thickness. The thinner the layer, the less resistence to mass transfer, consequently, larger mass transfer rates result. In Figure 2a for a 0.017mm radius bubble, large species outflow is apparent from the leading hemispherical bubble surface where the diffusion layer is very small. As flow proceeds toward the rear of the bubble, the diffusion layer thickens. When the diffusion layer approaches a very large thickness (the region sweeping a 30° arc of the diffusion tail directly behind the bubble) mass diffusion essentially stops. Figure 2b for a 0.13 radius bubble shows the rearward arc of the diffusion tail to close to approximately 15°. The diffusion is thinner in the leading edge region (though this can't be seen from the scale of the figures) and extends furtherback, hence, more mass transfer is occurring in Figure 2b than 2a. This is what one would expect since the convective velocities are significantly larger in Figure 2b than Figure 2a. Figure 2c, 0.47 radius bubble, extends this argument because an extremely thin diffusion layer exists almost entirely around the bubble. One can see that the faster the bubble rises, the thinner the diffusion layer becomes and the more it is pinned by the larger convective velocities at the bubble surface.

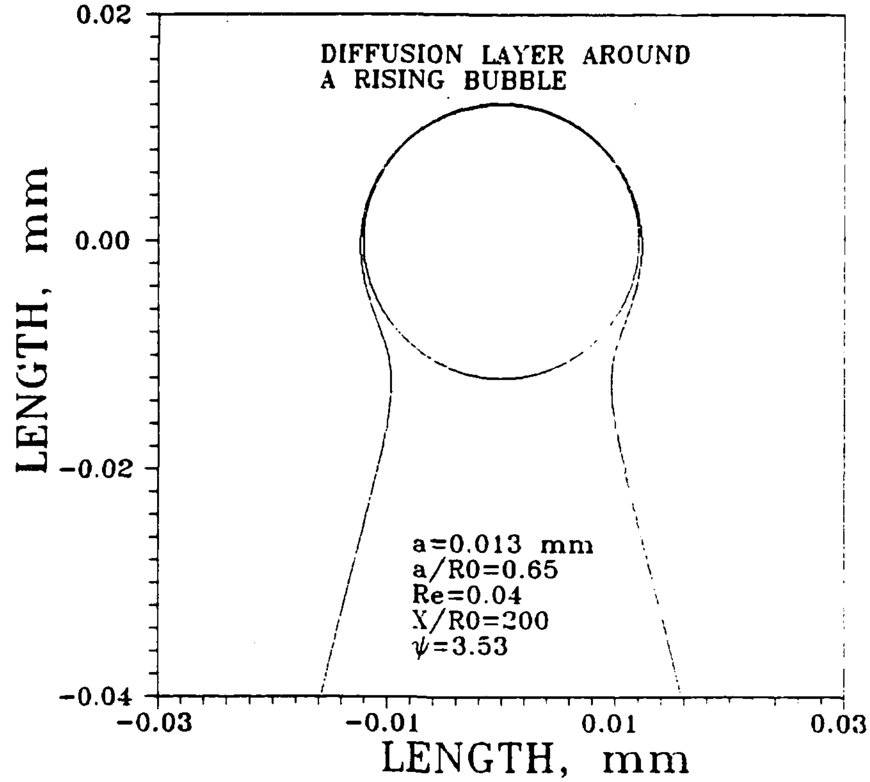

Figure 2a. Diffusion layer around rising bubble for Re=0.04.

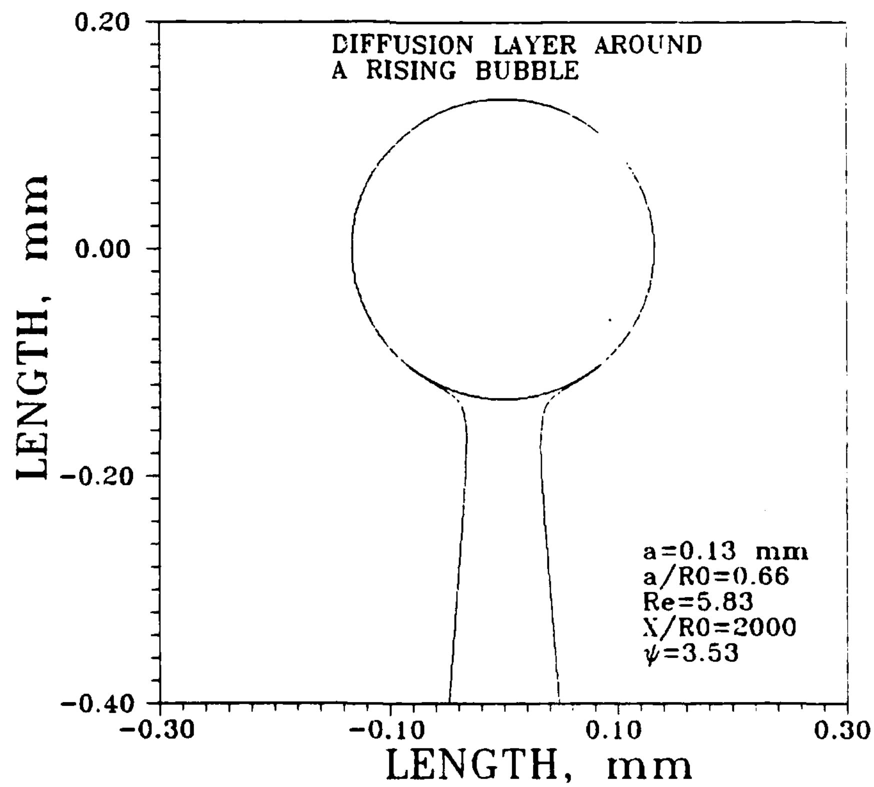

Figure 2b. Diffusion layer around rising bubble for Re=5.83.

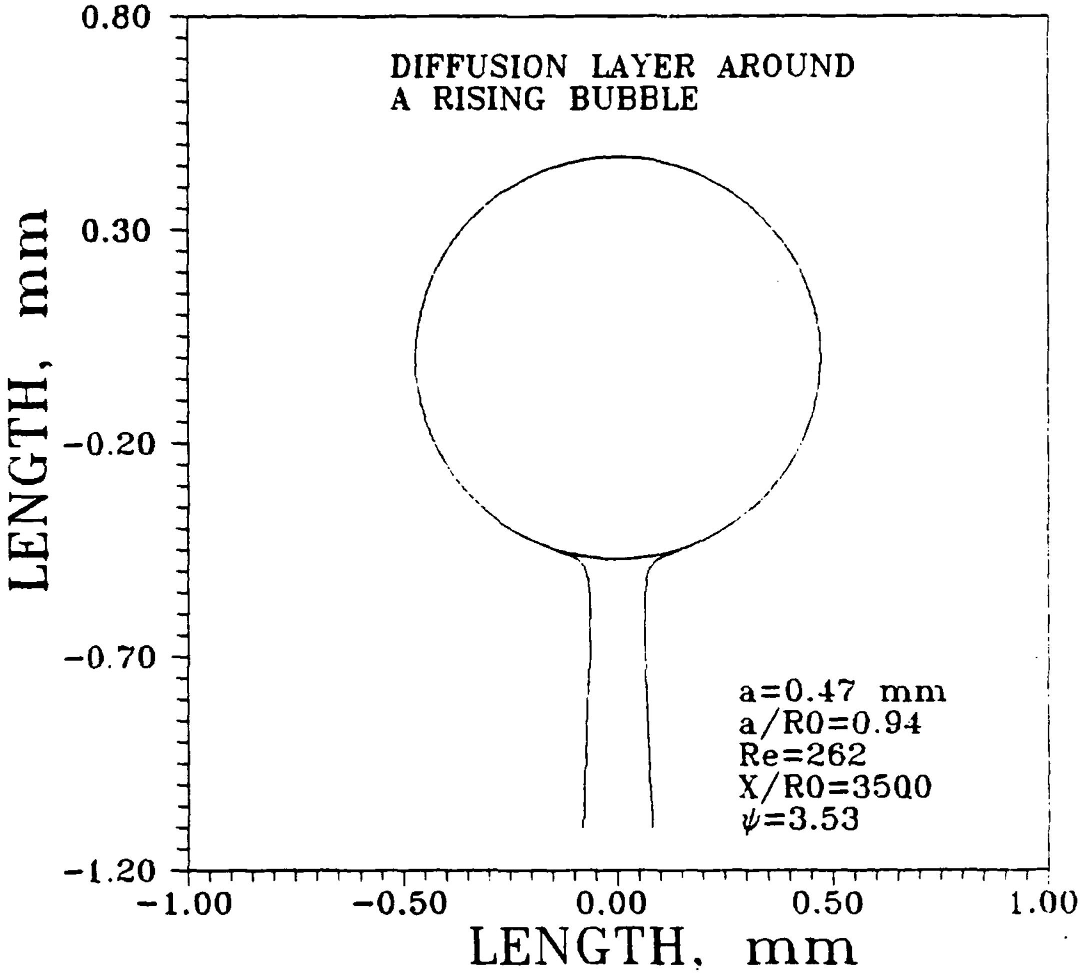

Figure 2c. Diffusion layer around rising bubble for Re=262.

Effect of Hydrostatic Head - Static Case.

Figures 3a and 3b represent the solution to eq. (29) for bubbles with initial radii of 0.50 and 0.20mm, respectively. The atmospheric $\Delta\ P$ for this case is zero. The ordinate represents the dimensionless radius based on initial bubble radius and the abscissa represents the dimensionless distance in the translational direction based on initial bubble radius. The solid curves represent eq. (29), and the dashed curves represent eq. (29) in the absence of the pressure gradient term, i.e. this would represent the case of a bubble translating in a constant pressure field. The curves in Figures 3a and 3b are also represented by the parameters ψ and β

where

$$\psi = (C_0 - C_s)\left(\frac{RT}{\gamma}\right)\left[\frac{D}{\pi\nu}\right]^{1/2},$$

$$\beta = \psi\frac{C_4}{aRe^{1/2}},$$

$$C_4 = \begin{cases} 2\sqrt{3}, & \text{slip-flow, Re}< 1 \\ 6, & \text{viscous dissipation, Re}>>1. \end{cases}$$

The parameter groupings ψ and β can most readily be seen by examination of eq. (35) with $C_3 = 0$. Eq. (35) can then be rearranged as follows,

$$\frac{da}{dt} = \frac{a}{3}\left(\frac{1}{P_b}\frac{dP}{dt}\right)[\beta + 1]. \qquad (35a)$$

ψ represents a collection of mass transfer parameters and β represents the ratio of the bubble volumetric change caused by mass transfer (diffusion) over the volumetric change caused by the time rate of change of the ambient pressure. Both terms were evaluated at their initial conditions, in reality, they would both continuously change during the time history for the rising bubble.

In Figure 3a, $a_0 = 0.50mm$, ψ equals 0 represents no bubble species loss via diffusion. This was achieved by setting the diffusion coefficent, D, equal to 0. A bubble with $\psi = 0$ will undergo a volumetric increase as it rises through a hydrostatic head because of the decreasing ambient pressure it encounters as it rises. Of course, the case of no change in pressure results in a straight horizontal line at $a/a_0 = 1.0$. The next pair of curves at $\psi = 2.38$ is representative of an air bubble rising in undersaturated water. The net result is a slow decrease in bubble volume as it rises towards the surface. A very strong diffusional loss can be seen at $\psi = 14.24$, $\beta = 10.0$. At $x/a_0 \approx 3500$, the bubble dissolves. The final curve, $\psi = 266.0, \beta = 1780$, shows very quick dissolution. This is representative of a CO_2 bubble in water. As can be seen by the series of curves on Figure 3a, when β gets very large, the effect of the ambient pressure change diminishes. This means that either a very large mass transfer loss and/or a very slow moving bubble (small bubble) causes the bubble to "see" a nearly constant pressure environment. As one can see in Figure 3b for a 0.20mm radius bubble, the effect of the pressure change due to a hydrostatic head is much less noticeable. Notice that in Figure 3b, the mass transfer constant ψ represents the same mass transfer parameters as in Figure 3a but the $\beta's$ are different because of both the smaller bubble size and , consequently, slower bubble rise velocity.

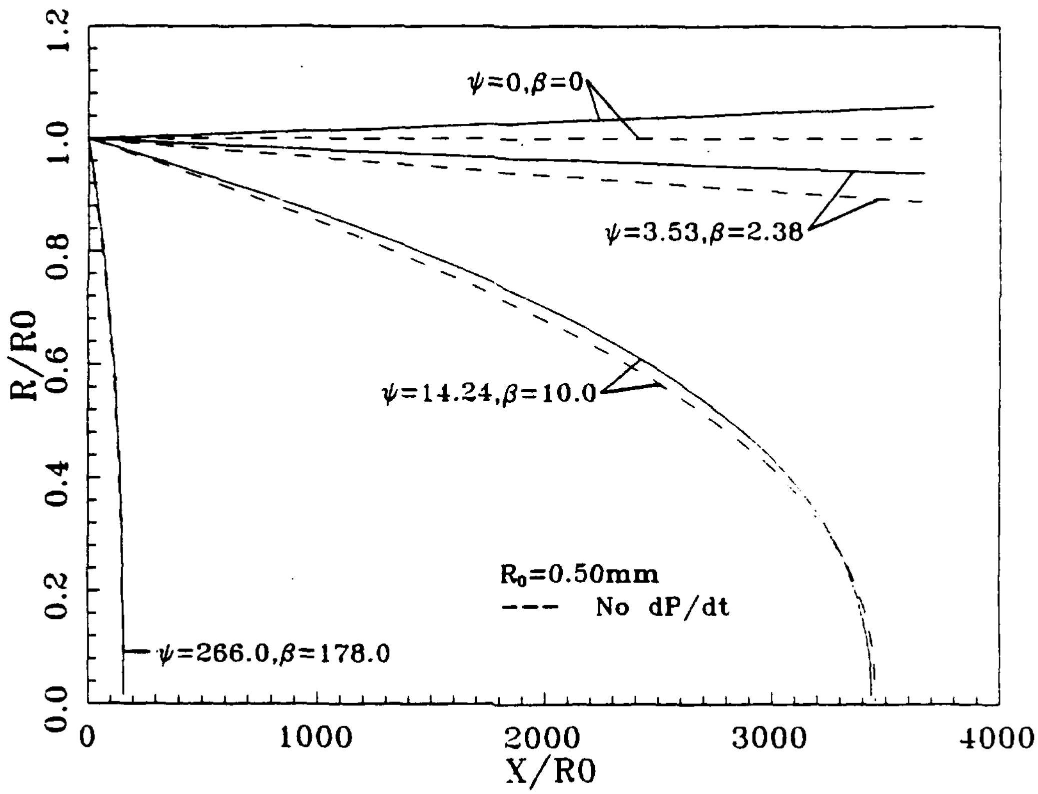

Figure 3a. Diffusion history of a rising 0.50mm radius bubble.

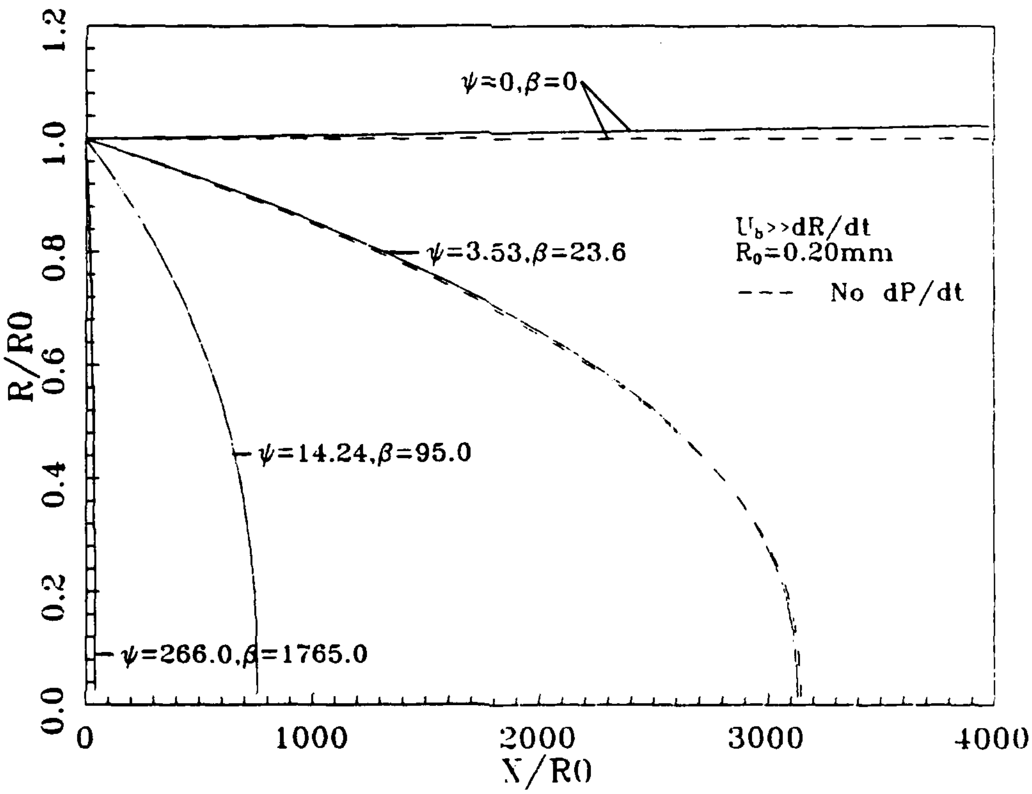

Figure 3b. Diffusion history of a rising 0.20mm radius bubble.

The effect of large bubble translation

When the bubble translational velocity is significantly larger than its radial velocity, eq. (35) greatly simplifies the numerical processing.

Figures 4a through 4c represent bubble rise in a hydrostatic head where the emphasis is on the comparison of eq. (29), with the model for significant translation, eq. (35). As can be seen, the simpler model Eq. (35), is quite accurate for bubbles larger than 0.02mm radius.

A comparison of convective vs. molecular diffusion models

A comparison of convective diffusion models and molecular diffusion models, i.e., no bubble translation, can be made by comparing the representative constituents of eq. (2),

$$V_r \frac{\partial C}{\partial r},$$

will be selected as the convective representative, and

$$D \frac{\partial^2 C}{\partial r^2},$$

will be chosen as the molecular representative.

The molecular diffusion term is included in the convective diffusion, eq. 2, since it defines the diffusion boundary layer thickness around the translating bubble. When the convective terms are excluded in eq. 2, the familar Epstein-Plesset equation for molecular diffusion from a stationary bubble results.

These terms can be non-dimensionalized as follows,

$$\frac{Pe}{r^*} \frac{\partial C^*}{\partial r^*} \sim \frac{\partial^2 C^*}{\partial r^{*2}} \tag{38}$$

where

$$r^* = r/a_0,$$

$$Pe = \frac{U_b a_0}{D},$$

and

$$C^* = \frac{C - C_0}{C_s - C_0}.$$

Then, if

$$\frac{\partial C^*}{\partial r^*} >> \frac{r^*}{Pe} \frac{\partial^2 C^*}{\partial r^{*2}}$$

convective diffusion predominates. This criterion can loosely translate to $\frac{U_b a_0}{D} >> 100$ for significant convective diffusion. Table I shows the minimum translational velocities for given air bubble radii in water where convective diffusion dominates.

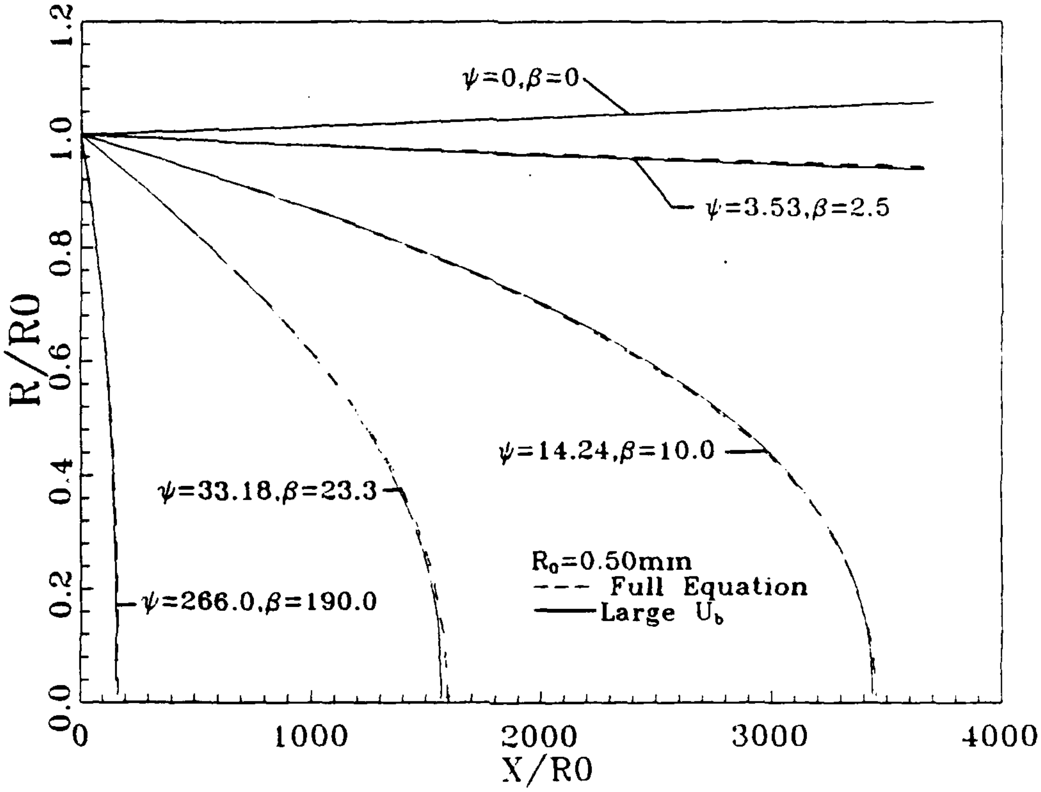

Figure 4a. Diffusion history of a rising 0.50mm radius bubble. Comparison of Eqs. 29 and 35.

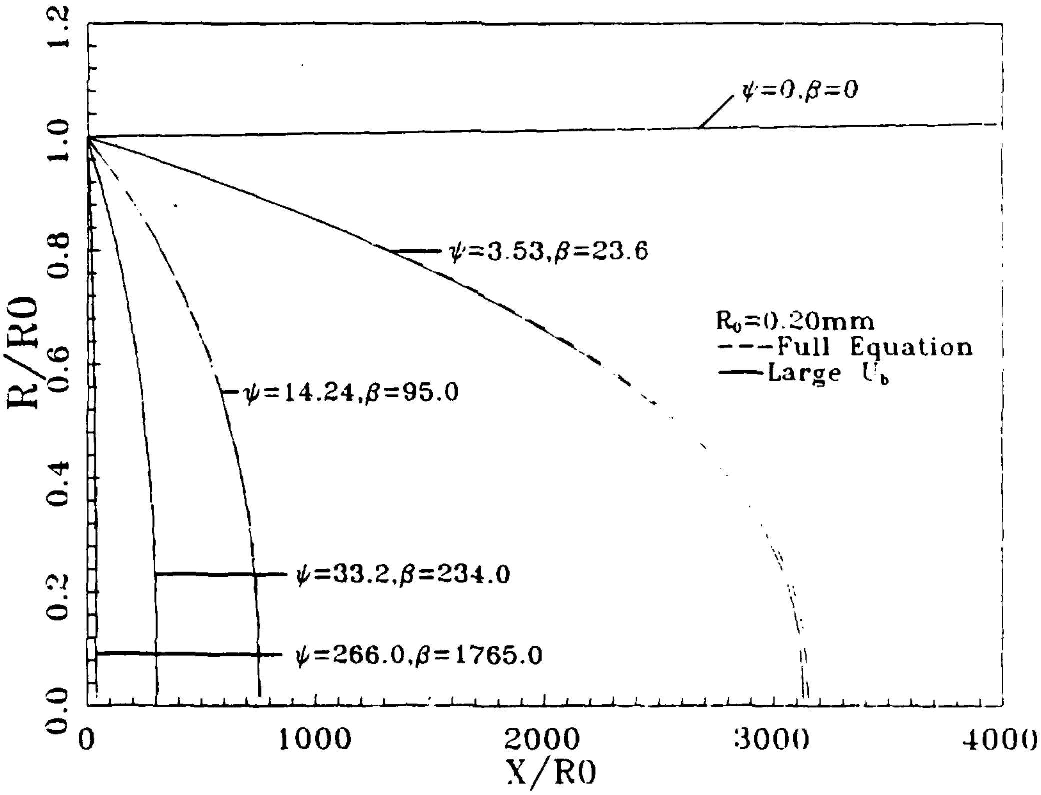

Figure 4b. Diffusion history of a rising 0.20mm radius bubble Comparison of Eqs. 29 and 35.

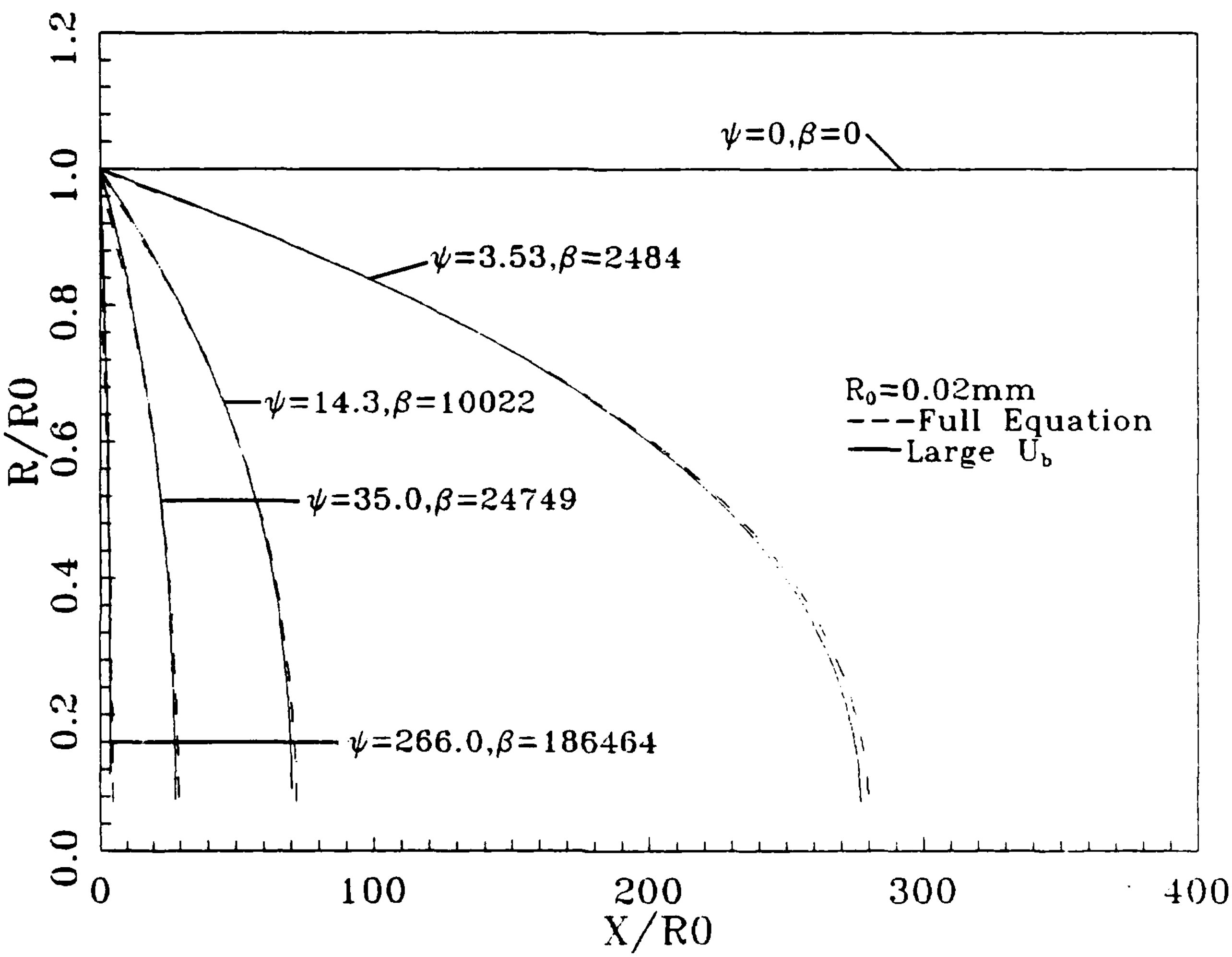

Figure 4c. Diffusion history of a rising 0.02mm radius bubble. Comparison of Eqs. 29 and 35.

Table I

Predominant Convective Diffusion, $D = 2x10^{-5} cm^2/s$

a_0, mm	U_b, mm/s
0.50	0.4
0.10	2.0
0.02	10.0
0.01	20.00

Figures 5a and 5b compare the convective diffusion model eq. (29) solid line, with the molecular diffusion model, dashed-line, of Epstein and Plesset [1]. As can be seen in Figure 5a for the bubble of initial radius size 0.20mm, the pure molecular diffusion model greatly underpredicts the radial history of the rising bubble. The reason for this is that molecular diffusion rates are much too small to account for the mass loss of the translating bubble which experiences large convective diffusion in this instance.

For the 0.02mm radius bubble case, Figure 5b, one can see that the convective diffusion effect is small compared to the molecular diffusion effect. This is shown by the fairly close agreement of the two models which signifies the small convective diffusion magnitude. At $\psi = 3.53$, initally there is a small convective effect imposed on the molecular diffusion effect as evidenced by the slightly faster bubble dissolution rate to about $a/a_0 = 0.5$. Then eq. (29) actually underpredicts the rising bubble dissolution history as evidenced by the crossing of the two models and the subsequent slower predicted bubble diffusion rate. The reason for this underprediction of eq. (29) compared to the Epstein-Plesset model is because in eq. (2) a portion of the molecular term was dropped to yield the approximated eq. (2a). At $\psi = 14.24$ the effect of this approximation is apparent. At $\psi = 266.0$, due to the very high diffusion potential which imparts a large radial velocity, the above mentioned effect diminishes slighty. In fact, the Epstein-Plesset model may be in error since their model does not incorporate a radial convective term in its formulation.

Decompression Case

Figures 6a and 6b represent a bubble rising in a hydrostatic head where the atmosphere above the hydrostatic head undergoes a decompression. Eq.(29) is employed with Eq. 10a. and is represented by the solid curves. The same cases for no mass loss, $\psi = 0$, are represented by dashed curves. The decompression amplitude above atmospheric pressure is $0.5atm$. Three different decompression time constants were modelled: $\tau = 0.10, \tau = 1.00$ and $\tau = 10.0s$. The case of $\tau = 0.10s$ represents the fastest decompression rate depicted on Figures 6. For the $\psi = 0.0$ and $\psi = 3.53$ cases an initial quick expansion is seen at x/a_0 approximately equal to 200 on Figure 6a and 20 on Figure 6b. This is due to the sudden atmospheric pressure "drop" above the hydrostatic head, thus, the bubble quickly expands. For the $\psi = 0.0$ case, the bubble then rises in the hydrostatic head and undergoes a slight volumetric expansion. For $\psi = 3.53$, once the volumetric expansion caused by the sudden drop in atmospheric pressure is over, diffusion sets in and the bubble starts to dissolve as it continues to rise in the water column.

At $\tau = 1.0s$ for $\psi = 0.0$ and $\psi = 3.53$, the initial volumetric expansion caused by the atmopheric pressure drop is less noticeable in Figure 6a, and non existent in Figure

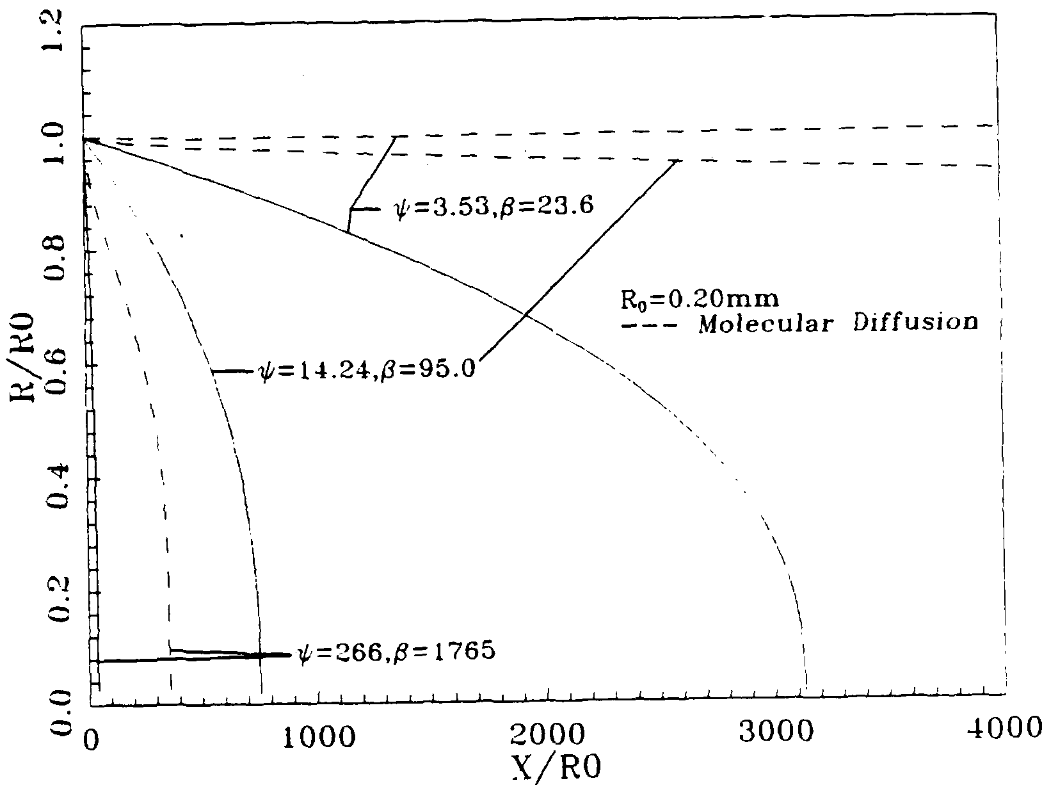

Figure 5a. Comparison of convective vs. molecular diffusion models for a rising 0.20mm radius bubble.

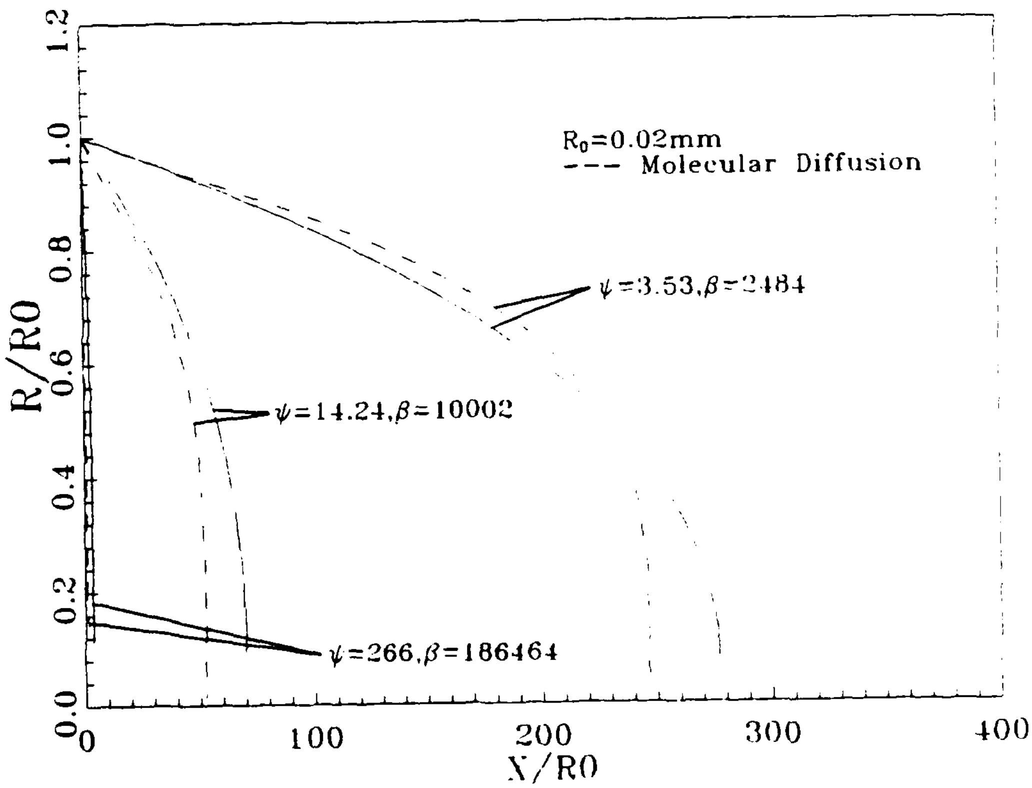

Figure 5b. Comparison of convective vs. molecular diffusion models for a rising 0.02mm radius bubble.

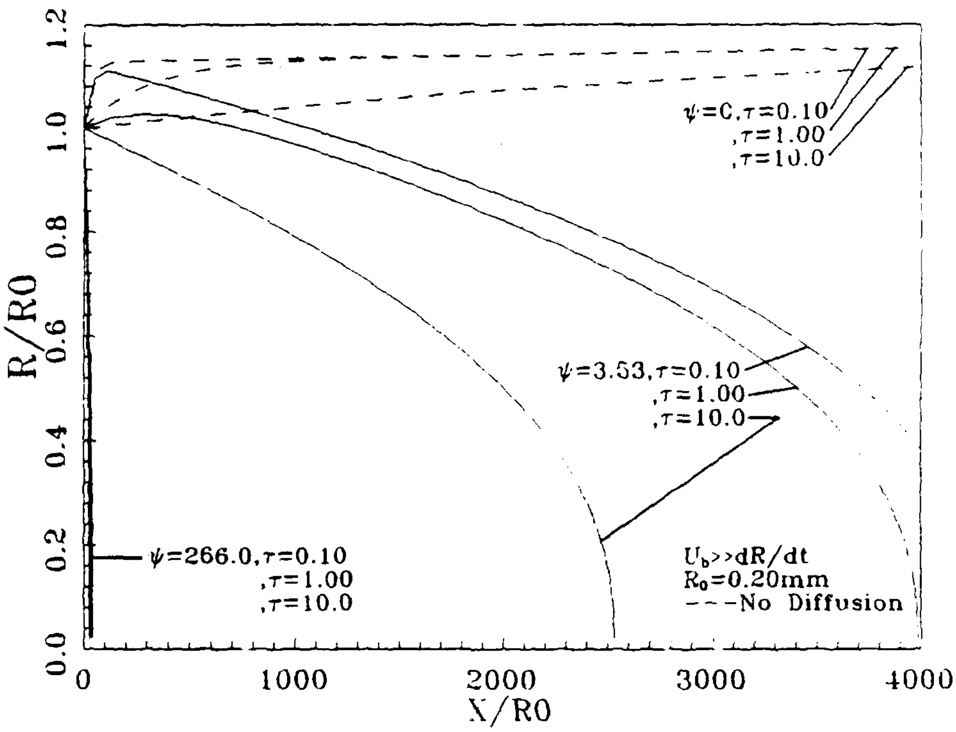

Figure 6a. Diffusion history for a rising 0.20mm radius bubble undergoing a decompression.

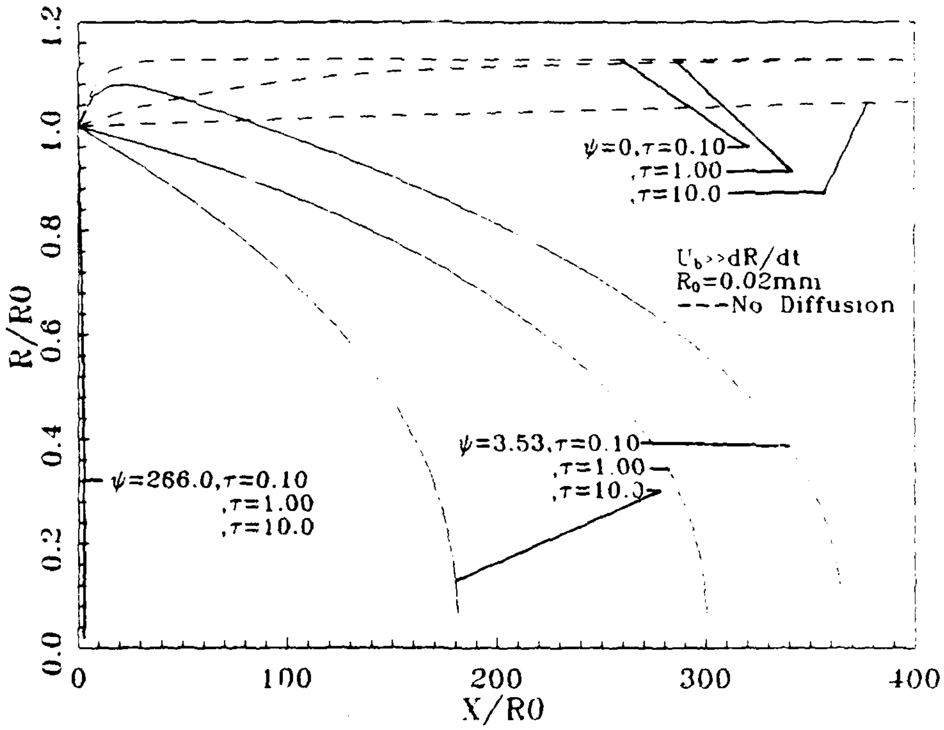

Figure 6b Diffusion history for a rising 0.02mm radius bubble undergoing a decompression.

6b for $\psi = 3.53$. This is due to the fact that the decompression process is slow enough to allow the diffusion processes to start to become effective. At $\psi = 0.0$, there is less of an initial volumetric expansion, but the bubble reaches the same total volumetric expansion as it did at $\tau = 0.10$ because there is no mass loss and the venting process is completely over. Since the processes started at and ended at the same beginning and end states, the approximately same volumetric end states should result, although the paths taken were different.

At $\tau = 10.0s$, the decompression process is very slow. For $\psi = 0.0$, the atmospheric end state of the other two cases is not reached during the x/a_0 represented on Figures 6a and 6b. For $\psi = 3.53$, the long decompression process allows diffusion to become significantly established and the bubble history is similar to that of previous cases.

At $\psi = 266.0$, the decompression rates used were relatively small compared to the initial high diffusion rates, hence, the bubbles were not affected by the decompression processes and they dissolved quickly.

The decompression model is an interesting case because it might represent what would occur to a bubble that was following a fluild streamline which would have an associated decrease in pressure during acceleration such as flow around a submerged body, or airfoil.

Oscillation case and rectified diffusion

Figure 7 represents the case of a bubble rising in a hydrostatic head where the atmosphere above the water column is oscillating at $1Hz$ with a pressure amplitude of $0.5atm$. The solid curves represent the oscillating case at various $\psi's$. The dashed lines represent the simple hydrostatic cases of eq. (29) for the same $\psi's$. At $\psi = 0.0$, no mass transfer occurs and the bubble oscillates as it rises to the surface. At $\psi = 3.53$, the bubble oscillates, but it is also losing mass through diffusion. This can be seen because the oscillation magnitude gets smaller and the bubble mean radius is decreasing until the bubble dissolves at x/a_0 equal to 3200. As the bubble oscillates in size it is also oscillating in velocity at this low frequency since the bubble velocity is approximately proportional the the radius squared. However, as mentioned earlier, if the bubble acceleration is too large during the oscillation process, eq. (29) might be invalid. This will be determined in a later section. As ψ increases to 14.24, the oscillation amplitude is seen to decrease at a faster rate since mass diffusion is higher and the bubble consequently gets smaller. At $\psi = 266.0$ there are no oscillations because the bubble has lost its mass via diffusion during the first oscillation pressure cycle.

There is the glimpse of an interesting phenomenon that occurs at $\psi = 3.53$ on Figure 7. It can be seen that the oscillating bubble dissolution history appears to be slightly slower than the case for no oscillation (dashed-line). This is seen by the slightly longer distance traveled before dissolution. One might think that the same dissolution histories should result. This discrepancy can be explained by arguments on rectified diffusion [21]. These will be summarized as follows:

When the bubble is small its internal pressure during an oscillation cycle is larger because the external pressure field is squeezing the bubble; thus, the concentration of species inside the bubble is higher (Henry's Law) than that during the expansion portion of the oscillation cycle; assuming that the ambient species concentration remains the same, the bubble, during the compression phase, will have a larger outgassing potential but a smaller

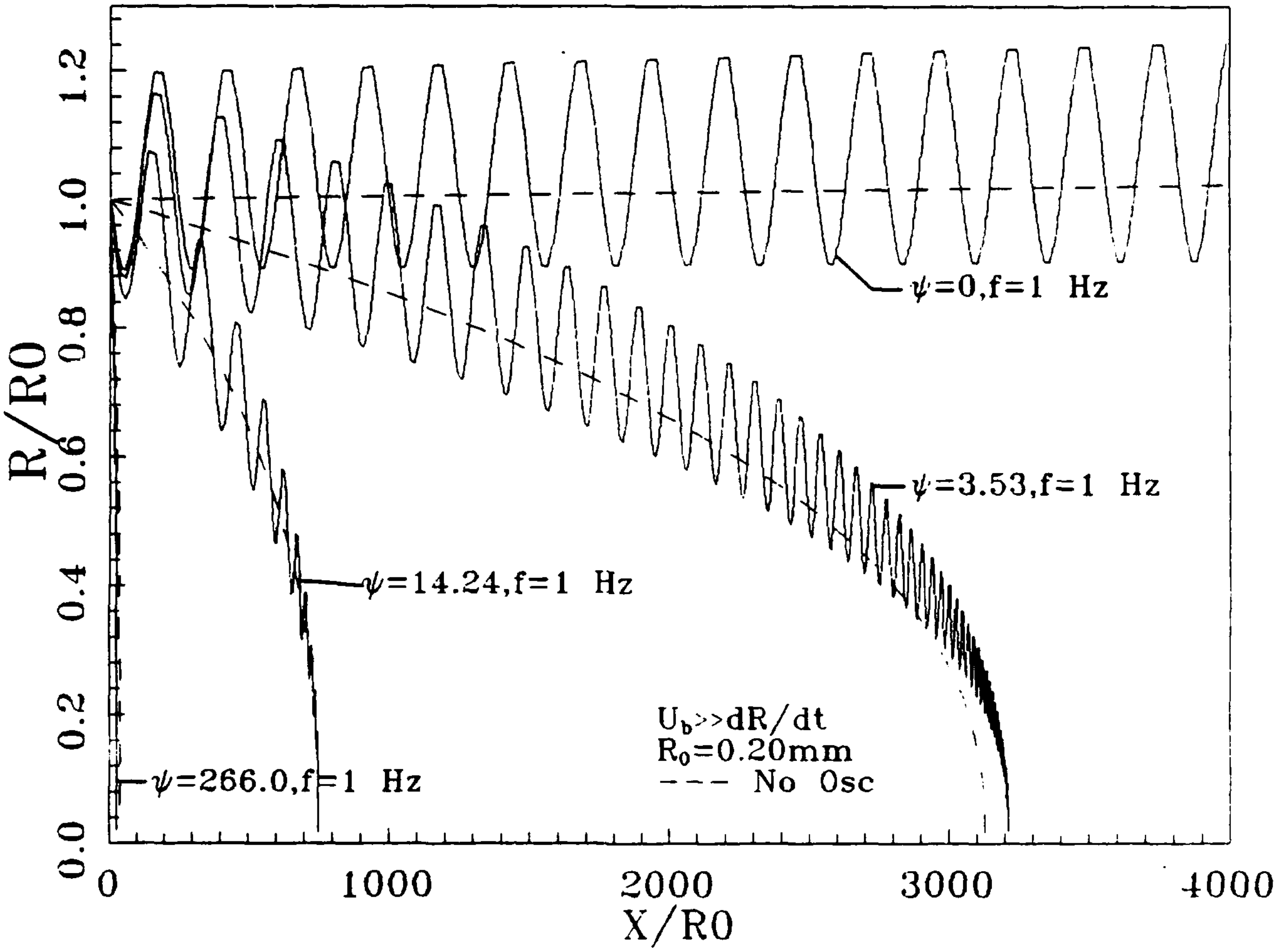

Figure 7. Diffusion history for a rising 0.20mm radius bubble undergoing a 1Hz oscillation.

outgas area; during the expansion phase, the bubble internal pressure is smaller, hence, the species concentration is smaller which results in a smaller dissolution rate through a larger surface area; the combination of smaller dissolution rate through a larger surface area signifies a smaller net dissolution rate over that of a non-oscillating bubble; the result is a bubble which dissolves more slowly than a bubble in a non-oscillating enviroment with the same physical properties.

The above argument is valid for a bubble which exists in an undersaturated solution below a specific rectified diffusion threshold which is property dependent. If the bubble lies in a saturated solution, the net effect during cycle oscillation would be species inflow, i.e., the bubble would grow because during the expansion portion of the cycle the species concentration inside the bubble would be lower than that outside and over many repeated oscillations the bubble would grow. This rectified diffusion phenomenon will not be dealt with any further in this study.

VALIDITY OF THE PSEUDO-STEADY MODEL

The presented model was based on the assumption of negligible bubble acceleration and resulted in the reduction of eq. (13) for Lagrangian motion to the simplified form, eq. (14). In this section we will test the validity of this assumption by comparing the order of magnitudes of the various terms in eq. (13) to the drag and buoyancy terms which are assumed to be of order 1.

Added mass loading

The first term on the right of eq. (13) represents the added mass loading. A ratio of added mass to bubble buoyancy therefore is

$$\frac{\frac{m_f}{2}\left(\frac{dU_b}{dt}\right)}{m_f g} = \frac{(dU_b/dt)}{2g}. \tag{39}$$

In the following analysis, the bubble acceleration brought about by changes in ambient pressure will be roughly estimated. This acceleration will then be introduced into eq. (39) and if the ratio is less than 5%, the acceleration reaction term will be deemed negligible. First, the assumption of slow mass transfer reduces the differentiated perfect gas law to

$$\frac{dP}{dt} = -(m_b RT)\frac{1}{V^2}\frac{dV}{dt}. \tag{40}$$

In terms of bubble radius, this can be rewritten as

$$\frac{dP}{dt} = -(m_b RT)\left(\frac{9}{4\pi}\right)\frac{da/dt}{a^4}. \tag{41}$$

In the presented pseudo-steady model, the assumption of

$$U_b = \frac{1}{3}\frac{g}{\nu}a^2$$

was made, where the coefficient for a fluid sphere ($Re < 1$) is used for this and the remainder analyses. The bubble acceleration can, therefore, be expressed as

$$\frac{dU_b}{dt} = \frac{2}{3}\frac{g}{\nu}a\frac{da}{dt}. \tag{42}$$

The combination of eqs. (41) and (42) results in

$$\left|\frac{dU_b}{dt}\right| = \frac{8}{27}a^5\frac{g}{\nu}\left(\frac{\pi}{m_bRT}\right)\left(\frac{dP}{dt}\right) = \left(\frac{2}{9}\right)\frac{g}{\nu}\frac{1}{P}\left(\frac{dP}{dt}\right)a^2. \tag{43}$$

The substitution of eq. (43) into eq. (39) then yields the following expression in order to neglect the acceleration reaction,

$$\frac{1}{9}\frac{a^2}{\nu}\frac{1}{P}\left(\frac{dP}{dt}\right) < .05, \tag{44}$$

where the pressure inside the bubble and its time derivative are given by eqs. (9) and (10), respectively. Note here that surface tension has been neglected. When eqs. (9) and (10) for the various cases are substituted into eq. (44) a series of inequalities which represent the validity of the various terms in eq. (13) result.

These are shown in Table II which represents data for an air bubble in 25C water. It should be pointed out that in the cases of pressure oscillations or decompressions, the various trigonometric or exponential terms were taken at their maximum or minimum values, whatever the case may be, to ensure the maximum value of eq. (44) in the construction of Table II. For brevity, the analyses for each case will not be presented here for they are only gross approximations. Table II shows that the acceleration reaction for a bubble rising in a simple hydrostatic head is practically non-existent for bubbles of spherical or prolate ellipsoid sizes, i.e., a 1mm diameter bubble has an Re of about 300 and will rise as a prolate ellipsoid. Acceleration reaction may be important, however, in the cases of pressure oscillations or decompressions where the bubble geometry may change quickly and significantly. For example, bubbles of 0.02mm and 0.20mm radii that are subjected to an oscillation pressure amplitude of 1/2 atm will have significant acceleration reaction for frequencies over 166 and 5 Hz, respectively. The same two bubbles at an overpressure of 1/2 atm above atmospheric will have significant acceleration reactions if the time constants for the decompression processes are less than 0.0003 and 0.01s, respectively, i.e., very rapid processes.

<u>"History" or B-B-O term</u>

The ratio of the history to buoyancy can be expressed as

$$\frac{3\sqrt{\frac{\nu}{\pi}}}{ag}\int_0^t \frac{[dU_b/d\tau]}{\sqrt{t-\tau}}d\tau. \tag{45}$$

Table II — Parameter Validity
(Air Bubble in 25°C Water)

	Simple Hydrostatic	Decompression	Oscillation
Acceleration Reaction	$a\,\mathrm{Re} < \begin{cases} 9305; & \mathrm{Re} < 1 \\ 27{,}900; & \mathrm{Re} >> 1 \end{cases}$	$\dfrac{a^2}{\tau\left(\dfrac{P_B}{\Delta P} + 1\right)} < \begin{cases} 0.418; & \mathrm{Re} < 1 \\ 1.254; & \mathrm{Re} >> 1 \end{cases}$	$\dfrac{a^2 f}{\left\lvert\left(\dfrac{P_B}{\Delta P} - 1\right)\right\rvert} < \begin{cases} 0.0665; & \mathrm{Re} < 1 \\ 0.200; & \mathrm{Re} >> 1 \end{cases}$
History	$\mathrm{Re}\, t^{1/2} < \begin{cases} 1426; & \mathrm{Re} < 1 \\ 4279; & \mathrm{Re} >> 1 \end{cases}$	$\dfrac{a t^{1/2}}{\tau\left(\dfrac{P_B}{\Delta P} + 1\right)} < \begin{cases} 0.064; & \mathrm{Re} < 1 \\ 0.192; & \mathrm{Re} >> 1 \end{cases}$	$\dfrac{a f t^{1/2}}{\left(\dfrac{P_B}{\Delta P} - 1\right)} < \begin{cases} 0.0102; & \mathrm{Re} < 1 \\ 0.0306; & \mathrm{Re} >> 1 \end{cases}$
Interfacial Movement	Negligible	$\dfrac{a^3 t^{1/2}}{\tau\left(\dfrac{P_B}{\Delta P} + 1\right)} < \begin{cases} 1.071; & \mathrm{Re} < 1 \\ 3.214; & \mathrm{Re} >> 1 \end{cases}$	$\dfrac{a^3 f^2 t^{1/2}}{\left(\dfrac{P_B}{\Delta P} - 1\right)} < \begin{cases} 0.0271; & \mathrm{Re} < 1 \\ 0.0814; & \mathrm{Re} >> 1 \end{cases}$

A conservative estimate for the magnitude of this ratio can be found by application of the maximum value theorem which when applied to eq.(45) results in

$$\frac{3\sqrt{\frac{\nu}{\pi}}}{ag}\int_0^t \frac{[dU_b/d\tau]}{\sqrt{t-\tau}}d\tau \le \frac{3\sqrt{\frac{\nu}{\pi}}}{ag}[dU_b/d\tau]_{max}\int_0^t \frac{1}{\sqrt{t-\tau}}d\tau. \qquad (46)$$

The evaluation of the integral in eq. (46), substitution of eq. (43) and 5% ratio limit results in

$$\frac{4}{3\sqrt{\pi\nu}}a\left[\frac{1}{P}\frac{dP}{dt}\right]_{max} t^{1/2} < .05 \qquad (47)$$

Table II shows the results of eq. (47) where eqs (9) and (10) have been used accordingly. For 0.02mm and 0.20mm radii bubbles rising in a simple hydrostatic head of approximately $1atm$, the history effect can be neglected for times up to about 2×10^6 and 203 s, respectively. The latter bubble has an initial velocity of approximately 46mm/s, if it did not diffuse and could maintain this velocity it would travel 9.3m before history effects would be noticeable. Hence, for small bubbles rising in a simple hydrostatic head, history effects are not apparent, unless their path lengths are extremely long such as bubbles rising from great depths toward the surface in the wake of a ship.

The same is not true, however, for the decompression or oscillation cases where bubble acceleration/decelerations may be more noticeable. If we take the 0.02 and 0.20mm radii bubbles as examples subject to an overpressure of $1/2atm$, at a decompression time constant of 1s the respective times for history effects to become apparent are 92 and 8.3 s. For a decompression process with a time constant of 0.1s, the time for noticeable history effects is less than 1s in both cases. Thus, the pseudo-steady model for the latter instance would not be appropriate. The oscillation case is even more dramatic. Oscillation frequencies as low as $1Hz$ coupled with high amplitudes of $1/2atm$ are still capable of providing fast bubble accelerations/decelerations. History effects would be apparent under these conditions for the 0.02 and 0.20mm bubble for times of 0.26 and 0.023 s, respectively. Therefore, the oscillation curves in Figure 7 may be somewhat in error.

Interfacial movement

The final ratio to be discussed deals with the amount of fluid momentum required to move the bubble interface, assuming that a free shear surface exists. If the bubble behaves as a solid body due to the accumulation of contaminents on its surface, this term would be zero. The ratio of interfacial movement to buoyancy is

$$\frac{a}{6\sqrt{\pi\nu g}}\int_0^t \frac{[d^2U_b/d\tau^2]}{\sqrt{t-\tau}}d\tau. \qquad (48)$$

Application of the maximum value theorem to pull the numerator out of the intergrand, subsequent expansion of the numerator term and using only the leading term from that expansion, results in the criteria shown in Table II. The results utilizing the same process parameters as before indicate that for small bubbles (0.02mm radius) interfacial momentum effects for a gas bubble in a heavy liquid are negligible. For larger bubbles (0.20mm radius)

there is a very slight effect for the decompression and oscillation cases, and no effect for the simple hydrostatic case.

CONCLUSIONS

A model for the diffusional growth or collapse of bubbles rising in time dependent pressure fields has been presented. The pressure fields that the model was subjected to included a simple hydrostatic head, a decompression hydrostatic head, and a hydrostatic head coupled to an oscillating reference pressure. The model itself was an extension of a model presented by Ruckenstein and Davis [11]. The model assumes a pseudo-steady approach through the neglect of added mass, history and interfacial momentum terms. Criteria are developed that allow the reader to determine the applicability of the pseudo-steady model for particular bubble diffusion problems.

Results of the model indicate that for small bubbles, the effect of the pressure gradient in a simple hydrostatic head is negligible. For bubbles larger than 0.50mm radius, there is an effect of pressure gradient in the simple hydrostatic case. An approximate model which neglects the bubble radial velocity is also developed to further facilitate computational time and the agreement with the full scale model is good. The convective model, is also compared to a molecular diffusion model and it is seen that even the slightest bubble translational motion greatly enhances the diffusion process, though this result is not new.

Finally, test cases representing decompression and oscillation pressure fields are shown and discussed. If the process is such that bubble acceleration/decelerations brought about by changes in bubble volume are small, the pseudo-steady model is accurate.

ACKNOWLEDGEMENTS

This work was accomplished at the Naval Research Laboratory while the first author held a National Research Council Postdoctoral Fellowship. The support of the ONR Code 1215 Surface Ship Wake Consortium also is acknowledged. The first author also wishes to acknowledge Dr. Steven E. Ramberg, now at ONR, who served as his advisor during the initial stages of the research.

REFERENCES

1. Epstein, P.S. and Plesset, M.S. "On the Stability of Gas Bubbles in Liquid-Gas Solution", J. Chem. Phys., Vol.18 No. 11, p. 1505, 1950.
2. Kirkaldy, J.J.,"The Time-Dependent Diffusion Theory for Condensation on Spherical and Plane Surfaces", Can. J. Phys., Vol. 36, p. 446, 1958.
3. Scriven, L.E.,"On the Dynamics of Phase Growth", Chem. Eng. Sci., Vol.10, p. 1, 1959.
4. Goodrich, F.C.,"On Diffusion-Controlled Particle Growth: The Moving Boundary Problem", J. Phys. Chem., Vol.70, p. 3660, 1966.
5. Haugton, G., Ritchie, P.D., and Thomson, J.A., Chem. Eng. Sci., Vol. 17, p. 221, 1962.
6. Wise, D.L. and Haugton, G., "The Diffusion Coefficients of Ten Slightly Soluble Gases in Water at $10 - 60°$ C", Chem. Eng. Sci., Vol. 21 p. 999, 1966.
7. Wise, D.L. and Haugton, G., "Diffusion Coefficients of Neon, Krypton, Zenon, Carbon Monoxide and Nitric Oxide in Water at $10 - 60°$ C", Chem. Eng. Sci., Vol.23, p. 1211, 1968.
8. Krieger, I.M., Mulholland, G.W., and Dickey, C.S., "Diffusion Coefficients for Gases in Liquids from the Rates of Solution of Small Gas Bubbles", J. Phys. Chem., Vol.71, p. 1123, 1967.
9. Gowing, S., "Dissolving of Bubbles in a Liquid", DTRC Report-87/006, 1987.
10. Ruckenstein, E., "Mass Transfer Between a Single Drop and a Continuous Phase", Int. J. Heat Mass Trans., Vol.10 p. 1785, 1967.
11. Ruckenstein, E. and Davis, E.J., "Diffusion-Controlled Growth or Collapse of Moving and Stationary Fluid Spheres", J. Coll. Int. Sci., Vol.34, p. 142, 1970.
12. Brankovic, A., Currie, I.G. and Martin, W.W., "Laser-Doppler Measurements of Bubble Dynamics", Phys. Fluids, Vol.27 p. 348, 1984.
13. Ishikawa, H., et al, "Gas Desorption from Liquids: Mass Transfer and Drag Coefficients for Single Bubbles in Free Rise Through Newtonian Liquids", Chem. Eng. Sci., Vol. 411, p. 2309, 1986.
14. Payvar, P., "Mass Transfer-Controlled Bubble Growth During Rapid Decompression of a Liquid", Int. J. Heat Mass Trans., Vol. 30, p. 699, 1987.
15. Happel, J., and Brenner, H., Low Reynolds Number Hydrodynamics, Martinus Nijhoff Publishers, Dordrecht, 1989.
16. Basset, A.B., A Treatise on Hydrodynamics, Vol.II, Dover, NY, 1961.
17. Morrison, F.A. and Stewart, M.B., "Small Bubble Motion in an Accelerating Liquid". ASME J.Appl. Mech., Vol.43, p. 399, 1976.
18. Levich, V.G., Physicochemical Hydrodynamics, Prentice Hall, Englewood Cliffs, NJ, 1962.
19. Hadamard, J., "Mouvement Permanent Lent d'une Sphere Liquide et Visqueuse dans un Liquide Visqueux", Comp. Rendus, Vol. 152, p. 1735, 1911.
20. Rybczynski, W., "Uber die Fortschreitende Bewegung einer Flussigen Kugel in einem zahen Medium," Bull. Int. de L'Academie des Sciences de Cracovie, p. 40, 1911.
21. Hsieh, D-Y and Plesset, M.S., "Theory of Rectified Diffusion of Mass into Gas Bubbles", J.Acous. Soc. Am., Vol.33, p. 206, 1961.